

NANO EXPRESS

Open Access

Optical properties of epitaxial BiFeO₃ thin film grown on SrRuO₃-buffered SrTiO₃ substrate

Ji-Ping Xu¹, Rong-Jun Zhang^{1*}, Zhi-Hui Chen², Zi-Yi Wang¹, Fan Zhang¹, Xiang Yu¹, An-Quan Jiang², Yu-Xiang Zheng¹, Song-You Wang¹ and Liang-Yao Chen¹

Abstract

The BiFeO₃ (BFO) thin film was deposited by pulsed-laser deposition on SrRuO₃ (SRO)-buffered (111) SrTiO₃ (STO) substrate. X-ray diffraction pattern reveals a well-grown epitaxial BFO thin film. Atomic force microscopy study indicates that the BFO film is rather dense with a smooth surface. The ellipsometric spectra of the STO substrate, the SRO buffer layer, and the BFO thin film were measured, respectively, in the photon energy range 1.55 to 5.40 eV. Following the dielectric functions of STO and SRO, the ones of BFO described by the Lorentz model are received by fitting the spectra data to a five-medium optical model consisting of a semi-infinite STO substrate/SRO layer/BFO film/surface roughness/air ambient structure. The thickness and the optical constants of the BFO film are obtained. Then a direct bandgap is calculated at 2.68 eV, which is believed to be influenced by near-bandgap transitions. Compared to BFO films on other substrates, the dependence of the bandgap for the BFO thin film on in-plane compressive strain from epitaxial structure is received. Moreover, the bandgap and the transition revealed by the Lorentz model also provide a ground for the assessment of the bandgap for BFO single crystals.

Keywords: BiFeO₃ thin film, Optical properties, Spectroscopic ellipsometry, Lorentz model, Dielectric function

PACS codes: 78.67.-n, 78.20.-e, 07.60.Fs

Background

BiFeO₃ (BFO) has attracted extensive research activities as an excellent multiferroic material. It simultaneously exhibits ferroelectricity with Curie temperature ($T_C = 1,103$ K) as well as antiferromagnetism with Neel temperature ($T_N = 643$ K), and the properties make BFO potential for applications in electronics, data storage, and spintronics [1,2]. Especially, the BFO thin film is paid much attention due to its large spontaneous polarization, which is an order higher than its bulk counterpart [3], and then the BFO thin film combined with nanostructures could be a promising candidate in the above applications [4]. In addition to its structural and electronic properties, optical properties of BFO thin films are focused on [5-9]. However, in the published literatures on optical studies, the BFO thin film is

usually directly deposited on perovskite oxide SrTiO₃ (STO) and DyScO₃ (DSO) substrate for epitaxial growth. So far, there is no report on optical properties of the BFO thin film with an electrode structure in spite of the fact that the lower electrode is necessary for the study on electronic and ferroelectric properties of the BFO thin film as well as for its applications including nonvolatile memory devices [10]. Since SrRuO₃ (SRO) is often chosen as the lower electrode for the BFO thin film as well as for the buffer layer to control its nanoscale domain architecture [11], it is desirable to investigate the optical properties of the BFO thin film grown on SRO.

Spectroscopic ellipsometry (SE) is a widely used optical characterization method for materials and related systems at the nanoscale. It is based on the measuring the change in the polarization state of a linearly polarized light reflected from a sample surface which consists of Ψ , the amplitude ratio of reflected *p*-polarized light to *s*-polarized light and Δ , the phase shift difference between the both [12]. The obtained ellipsometry spectra (Ψ and Δ at measured wavelength range) are fitted to the optical model for thin film nanostructure, and thus, rich

* Correspondence: rjzhang@fudan.edu.cn

¹Key Laboratory of Micro and Nano Photonic Structures, Ministry of Education, Shanghai Engineering Research Center of Ultra-Precision Optical Manufacturing, Department of Optical Science and Engineering, Fudan University, Shanghai 200433, China

Full list of author information is available at the end of the article

information including surface roughness, film thickness, and optical constants of nanomaterials are revealed [13,14]. Since SE allows various characterizations of the material, our group has studied some thin-film nanostructure using SE methods [15-18].

In this paper, we report the optical properties of epitaxial BFO thin film grown on SRO-buffered STO substrate prepared by pulsed-laser deposition (PLD) and measured by SE. The dielectric functions of STO, SRO, and BFO are extracted from the ellipsometric spectra, respectively. And the optical constants of the BFO thin film are obtained. The bandgap of 2.68 eV for the BFO thin film is also received and is compared to that for BFO thin film deposited on different substrate as well as BFO single crystals.

Methods

The epitaxial BFO thin film was deposited by PLD on SRO-buffered (111) STO single-crystal substrate. The SRO buffer layer was directly deposited on the STO substrate by PLD in advance. More details about the deposition process can be taken elsewhere [19]. The crystal phases in the as-grown BFO thin film were identified by X-ray diffraction (XRD, Bruker X-ray Diffractometer D8, Madison, WI, USA). The surface morphologies of the BFO thin film were investigated by atomic force microscopy (AFM, Veeco Instruments Inc., Atomic Force Microscope System VT-1000, Plainview, NY, USA). Both XRD and AFM investigation are employed to show growth quality of the BFO thin film for further optical measurement and analysis.

SE measurements were taken to investigate the optical properties of the BFO film. Considering the optical investigation with respect to a substrate/buffer layer/film structure, we should firstly obtain the optical response of the STO substrate and SRO buffer layer and then research the optical properties of the BFO thin film. The ellipsometric spectra (Ψ and Δ) were collected for the STO substrate, the SRO buffer layer, and the BFO film, respectively, at an incidence angle of 75° in the photon energy range of 1.55 to 5.40 eV by a SOPRA GES5E spectroscopic ellipsometer (Paris, France), as shown in Figure 1. Afterwards, the ellipsometric data, which are functions of optical constants and layer or film thickness, were fitted to the corresponding optical model depicted in the inset of Figure 1. By varying the parameters of the models in the fitting procedure, the root mean square error (RMSE) is expressed by [17]

$$\text{RMSE} = \sqrt{\frac{1}{2n-m-1} \sum_{i=1}^n \left[(\Psi_i^{\text{cal}} - \Psi_i^{\text{exp}})^2 + (\Delta_i^{\text{cal}} - \Delta_i^{\text{exp}})^2 \right]} \quad (1)$$

is minimized. Here, n is the number of data points in the spectrums, m is the number of variable parameters in the model, and 'exp' and 'cal' represent the experimental and the calculated data, respectively.

Results and discussion

The XRD pattern of the BFO film is displayed in Figure 2 and shows that a strong (111) peak of the BFO matches the closely spaced (111) ones of the SRO and STO, which

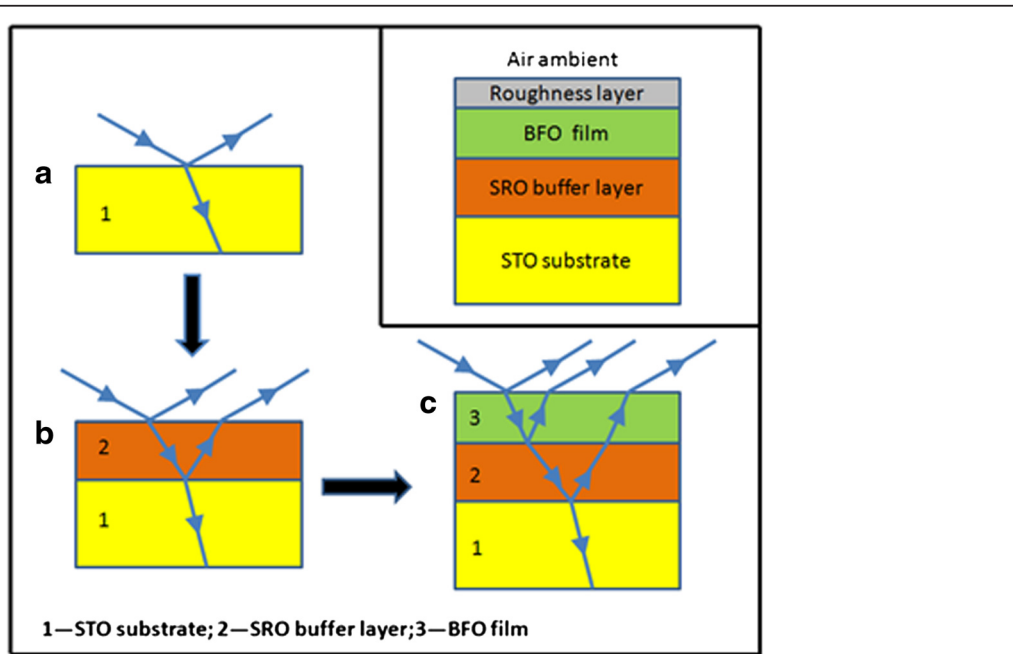


Figure 1 The schematic of SE measurements on BFO thin film with SRO buffer layer structure. (a) STO substrate, (b) SRO buffer layer, and (c) BFO film. The inset is the optical model of the BFO thin film on the SRO-buffered STO substrate.

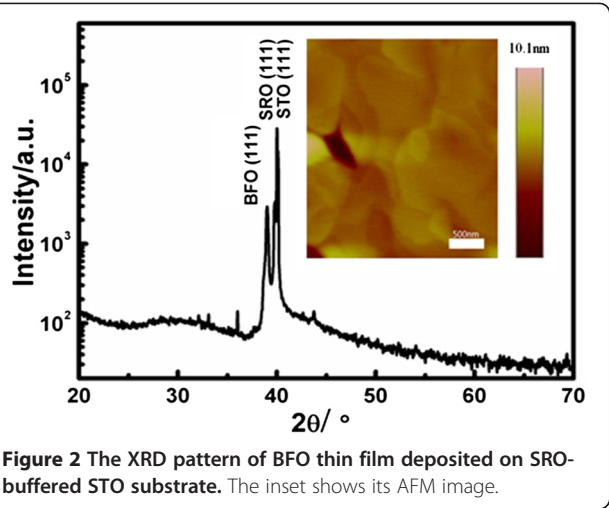


Figure 2 The XRD pattern of BFO thin film deposited on SRO-buffered STO substrate. The inset shows its AFM image.

demonstrates a well-heteroepitaxial-grown film that contains a single phase. As given in the inset of Figure 2, the epitaxial thin film deposited on the SRO/STO substrate is rather dense with R_q roughness of 0.71 nm. The XRD and AFM results together reveal a smooth epitaxial BFO thin film which is beneficial for the optical measurements.

The optical response of the STO substrate is calculated by the pseudo-dielectric function [20], and the obtained dielectric functions are shown in Figure 3a, which agrees well with the published literature [21]. The dielectric functions of SRO were extracted by minimizing the RMSE value to fit the ellipsometric data of the SRO buffer layer to a three-medium optical model consisting of a semi-infinite STO substrate/SRO film/air ambient structure. With the dielectric functions calculated for the substrate, the free parameters correspond to the SRO-layer thicknesses and a parameterization of its dielectric functions. The SRO dielectric functions are described in the Lorentz model expressed by [22].

$$\tilde{\epsilon} = \epsilon_{\infty} \left(1 + \sum_{j=1}^4 \frac{A_j^2}{(E_{center})_j^2 - E(E - i\nu_j)} \right) \quad (2)$$

The model parameterization consists of four Lorentz oscillators sharing a high-frequency lattice dielectric constant (ϵ_{∞}). The parameters corresponding to each oscillator include oscillator center energy E_{center} , oscillator amplitude A_j (eV) and broadening parameter ν_j (eV). This model yields thickness 105.15 nm for the SRO layer and the dielectric spectra displayed in Figure 3b. The center energy of the four oscillators is 0.95, 1.71, 3.18, and 9.89 eV, respectively, and is comparable to the reported optical transition for SRO at 1.0, 1.7, 3.0, and 10.0 eV [23,24], which indicates that the extracted dielectric functions are reliable.

The inset of Figure 1 sketches a five-medium optical model consisting of a semi-infinite STO substrate/SRO layer/BFO film/surface roughness/air ambient structure employed to investigate the BFO thin film where the roughness layer is employed to simulate the effect of surface roughness of the BFO film on SE measurement. Since the dielectric functions for the STO substrate and the SRO buffer layer as well as the thickness of SRO layer have been obtained, the free parameters correspond to the BFO film and surface roughness thicknesses and a parameterization of the BFO dielectric functions. The BFO dielectric functions are described by the same four-oscillator Lorentz model as the SRO layer. And the surface roughness layer is modeled on a Bruggeman effective medium approximation mixed by 50% BFO and 50% voids [25]. The fitted ellipsometric spectra (Ψ and Δ) with RMSE value of 0.26 show a good agreement with the measured ones, as presented in Figure 4. A BFO film of 99.19 nm and a roughness layer of 0.71 nm are yielded by fitting the ellipsometric data to the optical response from the above five-medium model. The roughness layer thickness is exactly consistent with the R_q roughness from the AFM measurement.

The obtained dielectric functions of the BFO thin film are given in Figure 5. In the Lorentz model describing the dielectric functions, the center energy of four oscillators are 3.08, 4.05, 4.61, and 5.95 eV, respectively, which matches well with the 3.09, 4.12, 4.45, and 6.03 eV reported from the first-principles calculation study on

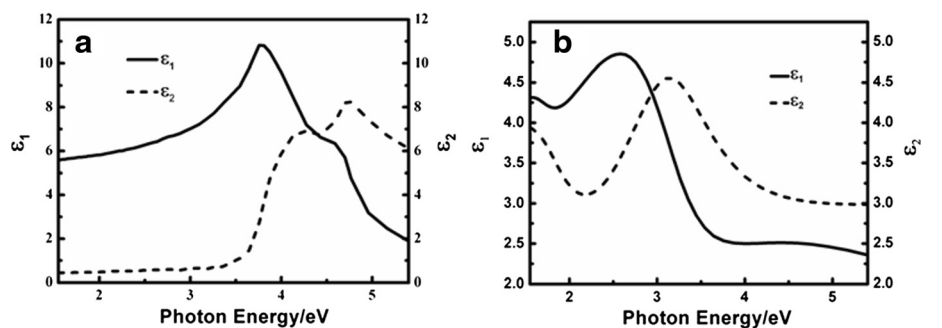


Figure 3 The dielectric functions for the STO substrate and SRO buffer layer. (a) STO substrate and (b) SRO buffer layer.

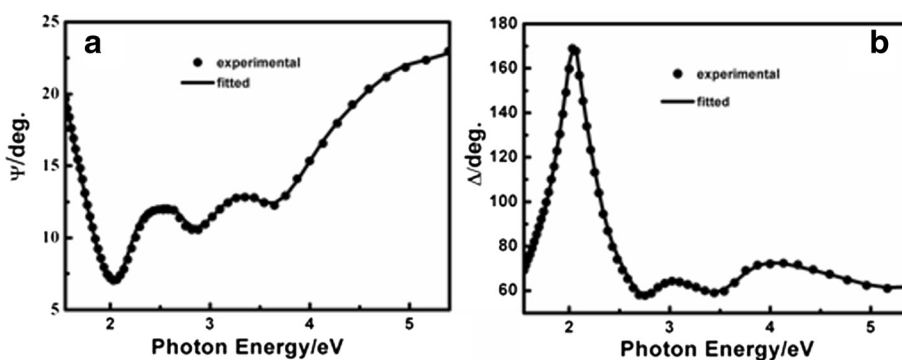


Figure 4 The measured and fitted ellipsometric spectra for the BFO film. (a) ψ and (b) Δ .

BFO [26]. The smallest oscillator energy 3.08 eV is explained either from the occupied O $2p$ to unoccupied Fe $3d$ states or the $d-d$ transition between Fe $3d$ valence and conduction bands while the other energies can be attributed to transitions from O $2p$ valance band to Fe $3d$ or Bi $6p$ high-energy conduction bands [26]. The optical constants refractive index n and extinction coefficient k are calculated through [27]

$$n = \left\{ \left[\varepsilon_1 + (\varepsilon_1^2 + \varepsilon_2^2)^{1/2} \right] / 2 \right\}^{1/2} \quad (3)$$

$$k = \left\{ \left[-\varepsilon_1 + (\varepsilon_1^2 + \varepsilon_2^2)^{1/2} \right] / 2 \right\}^{1/2} \quad (4)$$

and shown in Figure 6.

Plotting $(\alpha \cdot E)^2$ vs E where α is the absorption coefficient ($\alpha = 4\pi k/\lambda$) and E is the photon energy, a linear extrapolation to $(\alpha \cdot E)^2 = 0$ at the BFO absorption edge indicates a direct gap of 2.68 eV according to Tauc's principle, as shown in Figure 7a. In the plot of $(\alpha \cdot E)^{1/2}$ vs E displayed in Figure 7b, no typical indirect transitions are observed in the spectra range [28], suggesting that BFO has a direct bandgap. The bandgap 2.68 eV

obtained from the Lorentz model to describe dielectric functions of the BFO thin film is less than the reported 2.80 eV from the Tauc-Lorentz (TL) model [6]. Since the TL model only includes interband transitions [29], intra-band transitions and defect absorption taken account into the Lorentz model could impact the received bandgap. In addition, it is reported that there is photoluminescence emission peak at 2.65 eV for the BFO film ascribed to Bi^{3+} -related emission [30]. Thus, it is reasonable to believe that the near-band-edge transition contributes to our shrunk bandgap.

On the other hand, it deserves nothing that there is controversy about bandgap sensitivity of the epitaxial thin film to compressive strain from heteroepitaxial structure [5,7]. Considering that the degree of compressive stress imposed by the epitaxial lower layer progressively decreases with increasing BFO thickness [3], our result 2.68 eV from the BFO thin film prepared by PLD with a 99.19-nm thickness is compared to the reported ones of the BFO film on DSO or STO with comparable thickness as well as that deposited by PLD, as listed in Table 1.

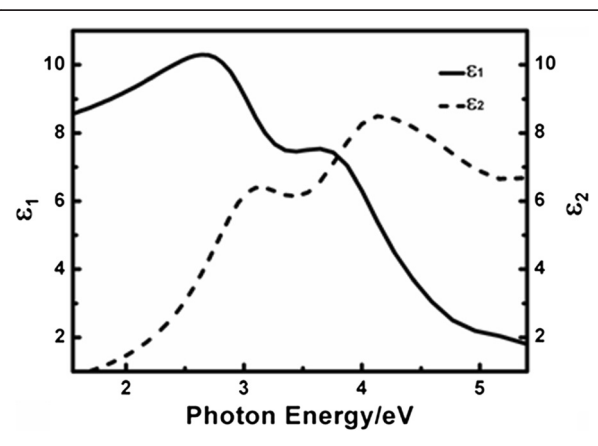


Figure 5 The real and imaginary parts of the dielectric function of the BFO thin film.

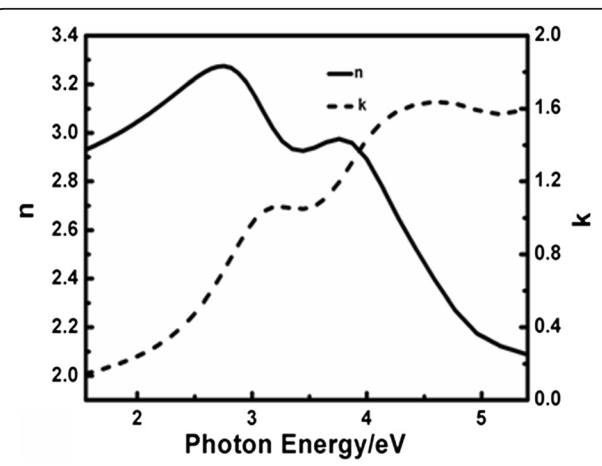


Figure 6 Refractive index n and extinction coefficient k of the BFO film.

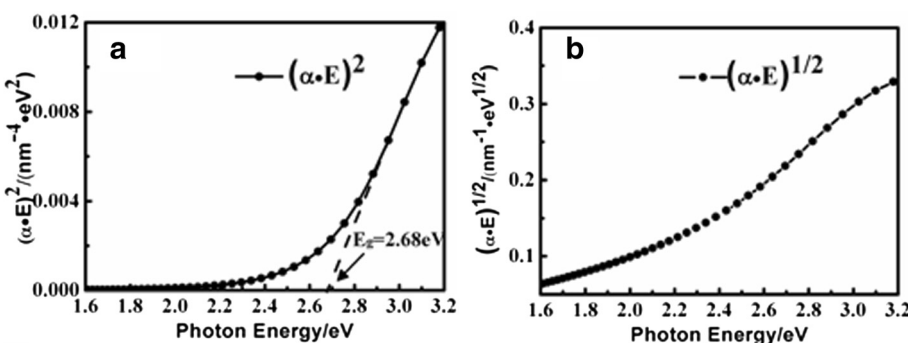


Figure 7 Plot of $(\alpha \cdot E)^n$ vs photon energy E . (a) $n = 2$ and (b) $n = 1/2$. The plots suggest that the BFO has a direct bandgap of 2.68 eV.

The bandgap of BFO on SRO is almost the same as that on DSO and is smaller than that on Nb-doped STO. It is noted that the in-plane (IP) pseudocubic lattice parameter for SRO and DSO is 3.923 and 3.946 Å [11], respectively, while STO has a cubic lattice parameter of 3.905 Å [7]. Considering the IP pseudocubic lattice parameter 3.965 Å for BFO [11], the compressive strain for the BFO thin film deposited on STO substrate is larger than that on SRO and DSO. Thus, the more compressive strain imposed by the heteroepitaxial structure, the larger bandgap for the BFO thin film, which agrees with the past report [7].

The obtained direct bandgap 2.68 eV of the epitaxial BFO thin film is comparable to 2.74 eV reported in BFO nanocrystals [31] but is larger than the reported 2.5 eV for BFO single crystals [32]. This can be understood because even for the epitaxial thin film, the existence of structural defect such as grain boundaries is inevitable, which will result in an internal electric field and then widen the bandgap compared to single crystals. On the other hand, a bandgap of 3 eV for BFO single crystals through photoluminescence investigation is also reported [33]. The broad and asymmetric emission peak at 3 eV in the photoluminescence spectra presented in [33] is attributed to the bandgap together with the near-bandgap transitions arising from oxygen vacancies in BFO. However, the Lorentz model employed to depict BFO optical response in our work reveals the existence of a 3.08-eV transition, which is the transition from the occupied O 2p to unoccupied Fe 3d states or the d-d transition between Fe 3d valence and conduction bands rather than the bandgap [26]. Therefore, the broad and

asymmetric peak is more likely to be explained as the overlap of the 3.08-eV transition and the bandgap transition with lower energy.

Conclusions

In summary, the optical properties of the epitaxial (111) BFO thin film grown on SRO-buffered STO substrate by PLD were investigated. The XRD and AFM analysis indicated that the BFO thin film sample is grown well with epitaxial structure and smooth surface. Then SE measurements were taken to get the ellipsometric spectra of the STO substrate, the SRO buffer layer and the BFO thin film, respectively, in the photon energy range 1.55 to 5.40 eV. The dielectric functions of STO, SRO, and BFO are obtained by fitting their spectra data to different models in which BFO corresponds to a five-medium optical model consisting of a semi-infinite STO substrate/SRO film/BFO film/surface roughness/air ambient structure. The BFO film and surface roughness thickness are identified as 99.19 and 0.71 nm, respectively. The optical constants of the BFO film are determined through the Lorentz model describing the optical response, and a direct bandgap at 2.68 eV is obtained which near-bandgap transitions could contribute to. Moreover, the gap value is compared to the BFO thin film with similar thickness deposited on various substrate prepared by PLD, indicating the dependence of the bandgap for the epitaxial BFO thin film on the in-plane compressive strain. In addition, the transition at 3.08 eV disclosed by the Lorentz model in our work suggests that the bandgap of BFO single crystals is less than 3 eV as previously reported. The results given in this work are helpful in understanding the optical properties of the BFO thin film and developing its application in optical field.

Table 1 Bandgap of BFO thin film (prepared by PLD) on different substrate

Bandgap (eV)	Substrate	Film thickness (nm)
2.68 (this work)	SRO-buffered STO	99.19
2.67 [8]	DSO	100
2.80 [7]	Nb-doped STO	106.5

Abbreviations

BFO: BiFeO₃; STO: SrTiO₃; DSO: DyScO₃; SRO: SrRuO₃; SE: spectroscopic ellipsometry; PLD: pulsed-laser deposition; XRD: X-ray diffraction; AFM: atomic force microscopy; RMSE: root mean square error; TL: Tauc-Lorentz; IP: in-plane.

Competing interests

We declare that we have no competing interests.

Authors' contributions

JPX carried out the optical measurements, analyzed the results, and drafted the manuscript. RJZ proposed the initial work, supervised the sample analysis, and revised the manuscript. ZHC grew the sample. ZYW and FZ performed the XRD and AFM measurements. XY helped dealing with the SE experimental data. AJQ helped the sample growth. YXZ, SYW, and LYC supervised the sample measurements. All authors read and approved the final manuscript.

Acknowledgements

This work has been financially supported by the National Natural Science Foundation of China (Nos. 11174058, 61275160, and 61222407), the No. 2 National Science and Technology Major Project of China (No. 2011ZX02109-004), and the STCSM project of China with Grant Nos. 12XD1420600 and 11DZ1121900.

Author details

¹Key Laboratory of Micro and Nano Photonic Structures, Ministry of Education, Shanghai Engineering Research Center of Ultra-Precision Optical Manufacturing, Department of Optical Science and Engineering, Fudan University, Shanghai 200433, China. ²State Key Laboratory of ASIC and System, School of Microelectronics, Fudan University, Shanghai 200433, China.

Received: 19 February 2014 Accepted: 11 April 2014

Published: 23 April 2014

References

- Catalan G, Scott JF: Physics and applications of Bismuth Ferrite. *Adv Mater* 2009, **21**:2463–2485.
- Neaton JB, Ederer C, Waghmare UV, Spaldin NA, Rabe KM: First-principles study of spontaneous polarization in multiferroic BiFeO₃. *Phys Rev B* 2005, **71**:014113.
- Wang J, Neaton JB, Zheng H, Nagarajan V, Ogale SB, Liu B, Viehland D, Vaithyanathan V, Schlom DG, Waghmare UV, Spaldin NA, Rabe KM, Wutting M, Ramesh R: Epitaxial BiFeO₃ multiferroic thin film heterostructures. *Science* 2003, **299**:1719–1722.
- Martin LW, Crane SP, Chu YH, Holcomb MB, Gajek M, Huijben M, Yang CH, Balken N, Ramesh R: Multiferroics and magnetoelectrics: thin films and nanostructures. *J Phys Condens Matter* 2008, **20**:434220.
- Ihlefeld JF, Podraza NJ, Liu ZK, Rai RC, Xu X, Heeg T, Chen YB, Li J, Collins RW, Musfeldt JL, Pan XQ, Schubert J, Ramesh R, Schlom DG: Optical band gap of BiFeO₃ grown by molecular-beam epitaxy. *Appl Phys Lett* 2008, **92**:142908.
- Kumar A, Rai RC, Podraza NJ, Denev S, Ramirez M, Chu YH, Martin LW, Ihlefeld J, Heeg T, Schubert J, Schlom DG, Orenstein J, Ramesh R, Collins RW, Musfeldt JL, Gopalan V: Linear and nonlinear optical properties of BiFeO₃. *Appl Phys Lett* 2008, **92**:121915.
- Himcinschi C, Vrejoiu I, Friedrich M, Ding L, Cobet C, Esser N, Alexe M, Zahn RT: Optical characterisation of BiFeO₃ epitaxial thin films grown by pulsed-laser deposition. *Phys Status Solidi C* 2010, **7**:296–299.
- Basu SR, Martin LW, Chu YH, Gajek M, Ramesh R, Rai RC, Xu X, Musfeldt JL: Photoconductivity in BiFeO₃ thin films. *Appl Phys Lett* 2008, **92**:091905.
- Xu XS, Brinzari TV, Lee S, Chu YH, Martin LW, Kumar A, McGill S, Rai RC, Ramesh R, Gopalan V, Cheong SW, Musfeldt JL: Optical properties and magnetochromism in multiferroic BiFeO₃. *Phys Rev B* 2009, **79**:134425.
- Liu X, Liu Y, Chen W, Li J, Liao L: Ferroelectric memory based on nanostructures. *Nanoscale Res Lett* 2012, **7**:285.
- Chu YH, Zhan Q, Martin LW, Cruz MP, Yang PL, Pabst GW, Zavaliche F, Yang SY, Zhang JX, Chen LQ, Schlom DG, Lin IN, Wu TB, Ramesh R: Nanoscale domain control in multiferroic BiFeO₃ thin films. *Adv Mater* 2006, **18**:2307–2311.
- Losurdo M, Bergmair M, Bruno G, Cattelan D, Cobet C, de Martino A, Fleischer K, Dohcevic-Mitrovic Z, Esser N, Galliet M, Gajic R, Hemzal D, Hingerl K, Humlcek J, Ossikovski R, Popovic ZV, Saxl O: Spectroscopic ellipsometry and polarimetry for materials and systems analysis at the nanometer scale: state-of-the-art, potential, and perspectives. *J Nanopart Res* 2009, **11**:1521–1554.
- Xia GQ, Zhang RJ, Chen YL, Zhao HB, Wang SY, Zhou SM, Zheng YX, Yang YM, Chen LY, Chu JH, Wang ZM: New design of the variable angle infrared spectroscopic ellipsometer using double Fourier transforms. *Rev Sci Instrum* 2000, **71**:2677–2683.
- Zhang RJ, Chen YM, Lu WJ, Cai QY, Zheng YX, Chen LY: Influence of nanocrystal size on dielectric functions of Si nanocrystals embedded in SiO₂ matrix. *Appl Phys Lett* 2009, **95**:161109.
- Zhao M, Zhang RJ, Gu HS, Chen MN: Preparation of (Ba_{0.5}Sr_{0.5})TiO₃ thin film by Sol-gel technique and its characteristics. *J Infrared Millim Waves* 2001, **20**:73–76.
- Zhao M, Zhang RJ, Gu HS, Xu JP: (Ba_{0.5}Sr_{0.5})TiO₃ thin film's preparation and its electric characteristics. *J Infrared Millim Waves* 2003, **22**:71–74.
- Chen YM, Zhang RJ, Zheng YX, Mao PH, Lu WJ, Chen LY: Study of the optical properties of Bi_{3.15}Nd_{0.85}Ti₃O₁₂ ferroelectric thin films. *J Korean Phys Soc* 2008, **53**:2299–2302.
- Zhang F, Zhang RJ, Zhang DX, Wang ZY, Xu JP, Zheng YX, Chen LY, Huang RZ, Sun Y, Chen X, Meng XJ, Dai N: Temperature-dependent optical properties of titanium oxide thin films studied by spectroscopic ellipsometry. *Appl Phys Express* 2013, **6**:121101.
- Chen ZH, He L, Zhang F, Jiang J, Meng JW, Zhao BY, Jiang AQ: The conduction mechanism of large on/off ferroelectric diode currents in epitaxial (111) BiFeO₃ thin film. *J Appl Phys* 2013, **113**:184106.
- Fujiwara H: Data analysis. In *Spectroscopic Ellipsometry: Principles and Applications*. Chichester: Wiley; 2007:147–208.
- Zollner S, Demkov AA, Liu R, Fejes PL, Gregory RB, Alluri P, Curless JA, Yu Z, Ramdani J, Droopad R, Tiwald TE, Hilfiker JN, Wollam JA: Optical properties of bulk and thin-film SrTiO₃ on Si and Pt. *J Vac Sci Technol B* 2000, **18**:2242–2254.
- Shen Y, Zhou P, Sun QQ, Wan L, Li J, Chen LY, Zhang DW, Wang XB: Optical investigation of reduced graphene oxide by spectroscopic ellipsometry and the band-gap tuning. *Appl Phys Lett* 2011, **99**:141911.
- Lee JS, Lee YS, Noh TW, Char K, Park J, Oh SJ, Park JH, Eom CB, Takeda T, Kanno R: Optical investigation of the electronic structures of Y₂Ru₂O₇, CaRuO₃, SrRuO₃, and Bi₂Ru₂O₇. *Phys Rev B* 2001, **64**:245107.
- Wang GT, Zhang MP, Yang ZX, Fang Z: Orbital orderings and optical conductivity of SrRuO₃ and CaRuO₃: first-principles studies. *J Phys Condens Matter* 2009, **21**:265602.
- Fujiwara H, Koh J, Rovira PI, Collins RW: Assessment of effective-medium theories in the analysis of nucleation and microscopic surface roughness evolution for semiconductor thin films. *Phys Rev B* 2000, **61**:10832–10844.
- Wang H, Zheng Y, Cai MQ, Huang H, Chan HLW: First-principles study on the electronic and optical properties of BiFeO₃. *Solid State Commun* 2009, **149**:641–644.
- Fujiwara H: Principles of optics. In *Spectroscopic Ellipsometry: Principles and Applications*. Chichester: Wiley; 2007:13–48.
- Basu PK: Interband and impurity absorptions. In *Theory of Optical Processes in Semiconductors*. Edited by Kamimura H, Nicholas RJ, Williams RH. Oxford: Clarendon; 1997:80–122.
- Jellison GE, Modine FA: Parameterization of the optical functions of amorphous materials in the interband region. *Appl Phys Lett* 1996, **69**:371–373.
- Chen X, Zhang H, Wang T, Wang F, Shi W: Optical and photoluminescence properties of BiFeO₃ thin films grown on ITO-coated glass substrates by chemical solution deposition. *Phys Status Solidi A* 2012, **209**:1456–1460.
- Yu X, An X: Enhanced magnetic and optical properties of pure and (Mn, Sr) doped BiFeO₃ nanocrystals. *Solid State Commun* 2009, **149**:711–714.
- Palai R, Katiyar RS, Schmid H, Tissot P, Clark SJ, Robertson J, Redfern SAT, Catalan G, Scott JF: β phase and γ - β metal-insulator transition in multiferroic BiFeO₃. *Phys Rev B* 2008, **77**:014110.
- Moubah R, Schmerber G, Rousseau O, Colson D, Viret M: Photoluminescence investigation of defects and optical band gap in multiferroic BiFeO₃ single crystals. *Appl Phys Express* 2012, **5**:035802.

doi:10.1186/1556-276X-9-188

Cite this article as: Xu et al.: Optical properties of epitaxial BiFeO₃ thin film grown on SrRuO₃-buffered SrTiO₃ substrate. *Nanoscale Research Letters* 2014 9:188.